Evaluating the influence of water table depth on transpiration of two vegetation communities in a lake floodplain wetland

Xiuli Xu, Qi Zhang, Yunliang Li and Xianghu Li

ABSTRACT

Groundwater plays an important role in supplying water to vegetation in floodplain wetlands. Exploring the effect of water table depth (WTD) on vegetation transpiration is essential to increasing understanding of interactions among vegetation, soil water, and groundwater. In this study, a HYDRUS-1D model was used to simulate the water uptake of two typical vegetation communities, *Artemisia capillaris* and *Phragmites australis*, in a floodplain wetland (Poyang Lake wetland, China). Vegetation transpiration was compared for two distinct hydrological conditions: high water table (2012) and low water table (2013). Results showed that vegetation transpiration in the main growth stage (July–October) was significantly influenced by WTD. Under high water table conditions, transpiration of *A. capillaris* and *P. australis* communities in the main growth stage totaled 334 and 735 mm, respectively, accounting for over 90% of the potential transpiration. Under low water table conditions, they decreased to 203 and 510 mm, respectively, due to water stress, accounting for merely 55% of the potential transpiration. Scenario simulations found different linear relationships between WTD and the ratio of groundwater contribution to vegetation transpiration. An increase of 1 m in WTD in the main growth stage may reduce the ratio by approximately 25%.

Key words | groundwater contribution, HYDRUS-1D, Poyang Lake wetland, vegetation transpiration, water table depth

Xiuli Xu
Qi Zhang (corresponding author)
Yunliang Li
Xianghu Li
Key Laboratory of Watershed Geographic Sciences,
Nanjing Institute of Geography and Limnology,
Chinese Academy of Sciences,
Nanjing 210008,
China
E-mail: *qzhang@niglas.ac.cn*

INTRODUCTION

Wetlands provide irreplaceable ecological values in supplying water resources, providing wildlife habitat, and maintaining biodiversity (Gilliam 1994; Baschuk *et al.* 2012). Despite the importance of these ecosystems worldwide, wetlands have been seriously threatened by droughts under the impacts of climate change and human exploitation (Mortsch 1998; Legesse *et al.* 2004; Candela *et al.* 2009). Wetland degeneration caused by water table drawdown, drying of rivers, and rainfall reduction has become an increasingly acute problem (Pattern *et al.* 2008; Zhang *et al.* 2008; Johansen *et al.* 2011). To protect these wetlands, better understanding is required of the mechanisms mediating hydrological processes and plant water use.

Water is fundamental for plant growth. It directly affects species germination, growth, and biomass accumulation (Fay & Schultz 2009). Rainfall, groundwater, and surface water are major water sources for vegetation transpiration. In areas with a shallow water table, upward movement of groundwater into the root zone plays an important role in supplying water to plants (Hurst *et al.* 2004; Satchithanantham *et al.* 2014). Previous studies focused on the effect of groundwater contributions to plant water use have been mainly conducted in arid regions (Yang *et al.* 2007; Zhu *et al.* 2009; Soylu *et al.* 2011); in humid areas, the role of

doi: 10.2166/nh.2016.011

groundwater has often been neglected, given the high level of rainfall. In fact, since the seasonal distribution of precipitation and transpiration are usually uneven, plants in humid areas may also experience water stress in the dry season when they have to depend heavily on other water sources for growth (Li *et al.* 2013; Blanken 2014).

Generally, wetland plants also experience periodic drought stress, especially in floodplains and river-connected lakes, as the habitat changes seasonally from aquatic to terrestrial environments due to variations of water table (Wilcox *et al.* 2002; Pagter *et al.* 2005). Water table depth (WTD) significantly influences vegetation water supply when wetlands change to terrestrial environments (Zhang & Schilling 2006; Xie *et al.* 2011), and WTD has been verified to be strongly related to vegetation characteristics at different scales. At the population scale, WTD significantly influences vegetation growth and morphology characteristics (Vretare *et al.* 2001). At the community scale, the distribution patterns of biomass and species richness have been found showing linear or unimodal relationships along WTD gradient (Dwire *et al.* 2006; Sorrell *et al.* 2012).

The aforementioned studies mainly focused on external plant characteristics in exploring the effect of WTD, while the internal processes, such as vegetation water use, have received less attention. As has been demonstrated, vegetation water use is one of the main processes resulting in adjustments in plant morphology and changes in distribution patterns (Chaves *et al.* 2003; Cooper *et al.* 2006; Muneepeerakul *et al.* 2008). In riparian and floodplain wetlands, groundwater is a significant water source for vegetation use (Mueller *et al.* 2005; Xie *et al.* 2011). Sanderson & Cooper (2008) reported that a wet meadow obtained about 75%–88% of its annual water requirement from groundwater, with mean daily depth ranging from 0 to 1.2 m in a floodplain wetland. In periodic flooded wetlands of the Laurentian Great Lakes, Mazur *et al.* (2014) found that groundwater varying within −0.1–0.6 m depth contributed 59%–75% of the annual evapotranspiration. A decline in the water table will directly reduce plant water use, and over the long term might result in vegetation succession. Zhang & Schilling (2006) reported that water use by *Phalaris arundinacea* decreased exponentially from 7.6 mm/d to zero as the water table declined from the ground surface to 1.42 m below ground in a floodplain wetland. In a riverine wetland in Colorado, Cooper *et al.* (2006) found that when a water table that ranged from 0.42 to 1.25 m depth was lowered to vary from 2.24 to 2.61 m in depth, a decrease of 32% of vegetation evapotranspiration resulted, leading to a consequent shift of dominant species from wetland grasses to shrubs.

The effects of groundwater availability on transpiration has been explored mostly in riverine wetlands where the water table varies typically within 3 m depth, and the effects occur primarily on grasses and meadow ecosystems (Kahlown *et al.* 2005; Yang *et al.* 2007; Sanderson & Cooper 2008), but knowledge is limited on the connections between groundwater and transpiration in wetlands with large variations in WTD, and little is known regarding the effects of these processes on mesophytes and hygrophytes. Upward fluxes of groundwater into the root zone depend on many factors, including WTD, soil hydraulic properties, vegetation types, evapotranspiration demand, and root development (Shah *et al.* 2007; Luo & Sophocleous 2010). Consequently, the response of different plants may differ in relation to various WTDs and soil conditions. The effect of water tables with large ranges of fluctuation on vegetation transpiration remains poorly understood.

Poyang Lake, the largest freshwater lake in China, is naturally connected to the Yangtze River (Liu *et al.* 2000). The lake water level fluctuates seasonally by up to 10 m under the influence of catchment inflows and discharge to/from the Yangtze River, which creates an approximately 3,000 km^2 grass-covered wetland (Li *et al.* 2014). Since over 55% of the precipitation in Poyang Lake falls from April to June, the upward flow of groundwater is crucial in satisfying plant water demand during the main growth period from July to October (Liu *et al.* 2000; Hu *et al.* 2010). However, over the past decade, drought events have occurred frequently in the lake (Lu *et al.* 2011; Zhang *et al.* 2012b). The high lake level (in July–August) is not as high as normal and the receding level (in September–October) is lower than normal (Min & Min 2010; Zhang *et al.* 2014).

Consequently, wetland vegetations are confronted with serious water stress, especially in autumn. Substantial degradation of upland communities was noted in Hu *et al.* (2010) and Zhong *et al.* (2014). The native area of *Artemisia capillaris* community showed some degree of desertification (Dronova *et al.* 2011; Zhou *et al.* 2011). In many of the alluvial

delta wetlands of inflow rivers, the distribution of the *Phragmites australis* community has shrunk dramatically, and some dominant hygrophytes have been replaced by xerophytes (Yu *et al.* 2010; Wu *et al.* 2010). These ecological problems are greatly threatening the biodiversity of the Poyang Lake wetland system, and have motivated a number of studies exploring the relationship between water level and vegetation. Studies have shown that at the landscape scale, vegetation distribution in Poyang Lake wetland is mainly shaped by WTD and inundation duration (Hu *et al.* 2010; Zhang *et al.* 2012a; Tan *et al.* 2016). At the local scale, vegetation biomass was revealed to follow a Gaussian model along WTD gradient (Xu *et al.* 2015). Although the above studies have highlighted the influence of WTD on vegetation growth characteristics in Poyang Lake, questions remain regarding the effect of WTD on vegetation transpiration. In particular, exactly how the groundwater contribution to vegetation transpiration changes along with a decline in the water table is poorly understood.

Mathematical models are important tools that can be used to quantify wetland water movement under a wide range of conditions and scenarios (Schlegel *et al.* 2004; Xie *et al.* 2011). There are mainly two types of wetland models: conceptual models and mechanistic models. Conceptual models were popularly used for wetland water balance assessment by treating the study area as a whole and ignoring the internal physical processes (Hussey & Odum 1992; Deng *et al.* 2003). Comparatively, the mechanical models, based on the Darcy law and continuity equation, can describe the water movement processes more accurately. A number of specific wetland models, e.g., the WETLAND and MIKE-SHE, have been widely used to describe the processes of overland flow, subsurface flow, and channel flow in depressions and river riparian wetlands at regional scales (Refsgaard & Storm 1995; Mansell *et al.* 2000; Zhang *et al.* 2008; Hammersmark *et al.* 2009). Other mechanical models, such as SWAP and HYDRUS, are effective in simulating interface water movement through the soil–plant–atmosphere system at field scales (Deng & Hu 2003; Li *et al.* 2011). The HYDRUS-1D model (Šimůnek *et al.* 2008), for instance, is a widely used model for exploring water flow transport in variably saturated profiles. It has been successfully applied in many ecosystems, e.g., croplands, river riparian wetlands, and seasonally flooded wetlands, due to its adaptability and flexibility (Jimenez-Martinez *et al.* 2009; Xie *et al.* 2011).

Thus, in this study, the above-referenced HYDRUS-1D model was used to simulate water movement through the groundwater–soil–plant–atmosphere continuum and assess the effect of WTD on transpiration of two Poyang Lake wetland vegetation ecotypes: *A. capillaris* and *P. australis* communities. The main objectives of this study were: (1) to compare vegetation transpiration of two communities in two distinct hydrological years representing high and low water table conditions; and (2) to quantitatively explore the effect of WTD on the groundwater contribution to transpiration.

MATERIALS AND METHODS

Study site

In this study, an alluvial delta wetland zone of the west branch of the Ganjiang and Xiushui Rivers was selected as an experimental site (116°00′11″ E, 29°14′34″ N). The site was located within the Poyang Lake National Nature Reserve (Figure 1(a)). It is the most typical delta wetland in Poyang Lake among other alluvial delta wetlands, such as the central and south branches of the Ganjiang and Fuhe Rivers' delta zone, and the Raohe River delta zone (Yu *et al.* 2010; Wu & Liu 2015). The wetland declines from the upland of the Ganjiang River levee to the lowland adjacent to the lake, with elevation decreasing from 18 to 12 m (Wusong Datum) (Figure 1(b)). Wetland vegetation communities, *A. capillaris*, *P. australis*, and *Carex cinerascens* communities grow best and are zonally distributed along the topographical gradient. The site undergoes seasonal inundation associated with the intra-annual lake water level variations. The *A. capillaris* community is distributed at the highest elevation area (17–18 m), which is flooded for less than 1 week. The *P. australis* community occurs at the middle–high elevation (14–16 m), and is subject to flooding for approximately 1–2 months (July–August) during a year. In this study, the upland wetland vegetation, *A. capillaris* and *P. australis* communities, which represent the mesophyte and hygrophyte, separately, were selected as subjects for field experiments (Figure 1(b)). These two communities have been found to be most vulnerable to

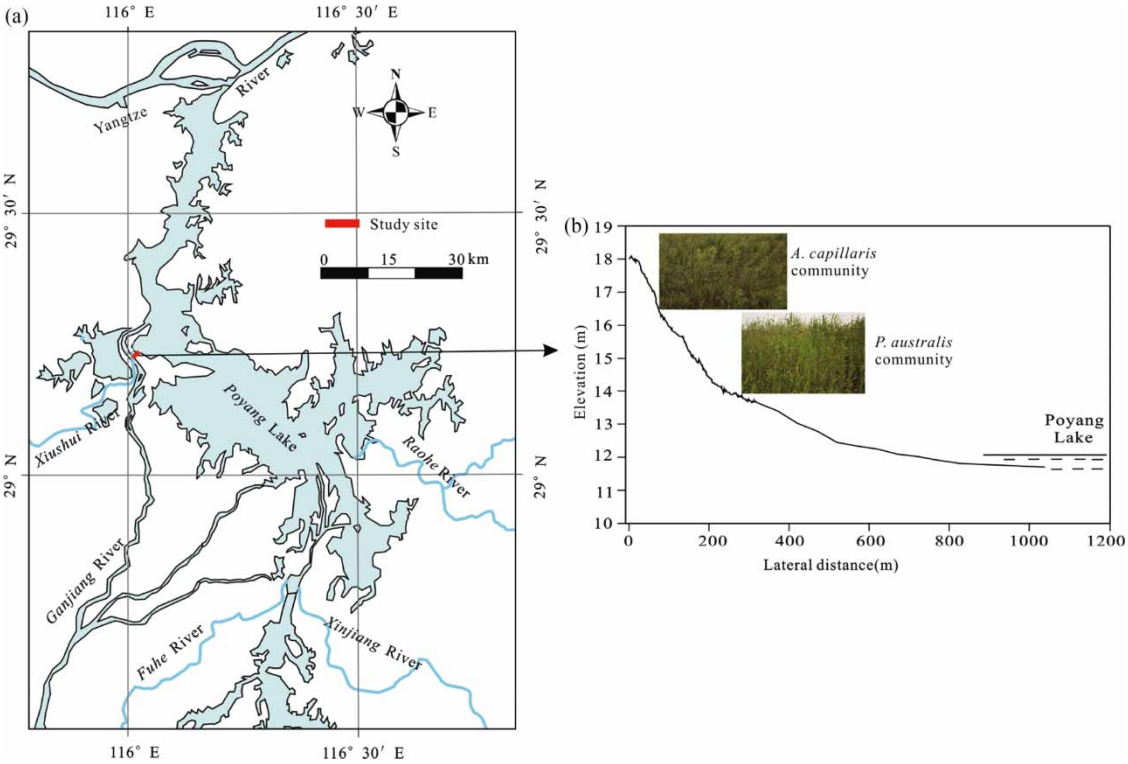

Figure 1 | Location of the study site in the Poyang Lake wetland (a) and the distribution of studied wetland vegetation communities (b).

water level changes, as noted in a number of previous studies (Wu & Ji 2002; Hu *et al.* 2010; Yu *et al.* 2010).

The region possesses a subtropical humid monsoon climate with an average annual temperature of 17 °C. Annual precipitation averages approximately 1,400 mm, with over 55% falling during the wet season from April to June (Liu *et al.* 2000). During the study period, the annual rainfall in the study site was 1,640–1,745 mm, with nearly 60% falling from March to June (Figure 2(a)). Average annual evapotranspiration is approximately 1,080 mm, with the highest values from July to October accounting for about 55% of the annual amounts (Liu *et al.* 2000). The seasonal distribution of rainfall and evapotranspiration is significantly different.

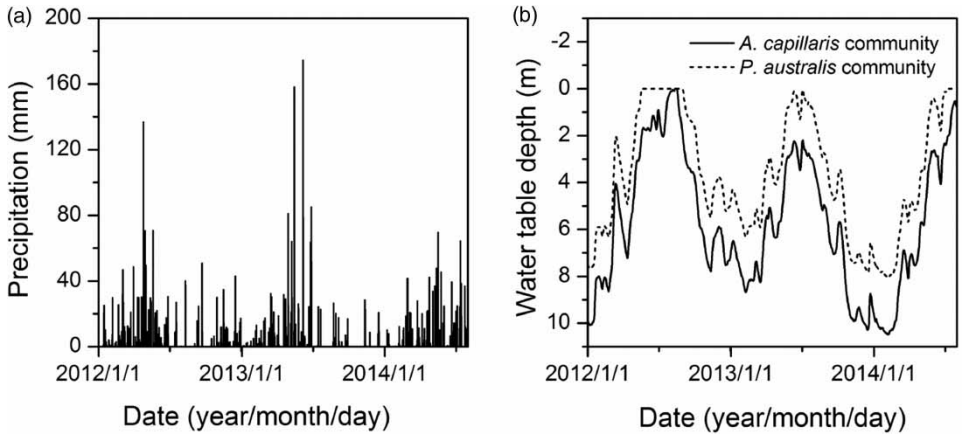

Figure 2 | Daily variations of precipitation (a) and WTD (b) measured from January 2012 to July 2014.

The water table in this site varies following the seasonal pattern of the water level in Poyang Lake (Xu *et al.* 2014). It generally rises above the ground surface in high water periods (July–August) and decreases to approximately 10 m below ground in low water periods (January–February) (Figure 2(b)). The water table in 2012 was significantly higher than in 2013. In the *A. capillaris* community, the highest water table level in 2012 almost reached the ground surface, but was at 2.2 m below ground in 2013. In the *P. australis* community, the land was flooded from May 17 to August 31 in 2012, during which time the groundwater table remained above the ground surface; however, in 2013 the highest water table never reached the ground surface. Therefore, the water level conditions in 2012 and 2013 represent high and low water table conditions, respectively.

The soil texture is mainly sand in the *A. capillaris* community and silt in the *P. australis* community, with mean soil bulk density of 1.33 g cm^{-3} at 0–100 cm depth. The *A. capillaris* community is mainly composed of mesophytic species of *A. capillaris*, *Cynodon dactylon*, *Eriophorum angustifolium*, and *Hemarthria altissima*. The *P. australis* community is composed of hygrophytes, including *P. australis*, *Triarrhena lutarioriparia*, and *Artemisia selengensis*. The upland wetland plants, e.g., the *A. capillaris* community, usually have one growing season. They germinate in March, thrive during April–August, blossom during September–October, and wither after the middle of December. For the middle–high wetland vegetation, e.g., the *P. australis* community, emergent plants usually grow fast out of the water when the land is flooded in July–August and have some re-germination after flooding again. Additionally, based on annual vegetation sampling results, the total biomass of the *A. capillaris* and *P. australis* communities both peaked in July–September (Xu *et al.* 2015). Thus, the periods during April–June and July–October are, respectively, defined as the initial and main growth stages for the upland wetland vegetation (Liu *et al.* 2000).

Data availability

Hydrological data

At the center of each community, volumetric soil moisture within the root zone was monitored at depths of 10, 50, and 100 cm by automatic probes (MP406 loggers, LSI-LASTEM, Italy). Next to the soil moisture sensors, one groundwater observation well was installed. Groundwater level was measured by a water pressure sensor (DQC001, LSI-LASTEM) installed inside the well. All the sensors were installed in December 2011 and the data were recorded daily from January 1, 2012 to July 31, 2014.

Meteorological data

A micro-meteorology station was established to measure daily meteorological data at the study site, including rainfall, solar radiation, humidity, wind speed, and the maximum and minimum air temperature.

A Bowen ratio-energy balance (BREB) system (SP300, LSI-LASTEM) was constructed in December 2012 to estimate evapotranspiration in the *A. capillaris* community. The lower and upper probes for temperature and humidity (DMA672.1, LSI-LASTEM) were positioned 1.2 and 2.5 m above the ground surface, respectively. Net radiation was measured by a net radiometer (DPA240, LSI-LASTEM) positioned at 3 m above ground. Soil heat flux was measured by two soil heat flux plates (HFP01, LSI-LASTEM) buried 10 cm deep. Soil temperature was also measured using a thermocouple probe (TM10 K, LSI-LASTEM) at a depth of 10 cm. Measurements were made every 10 min from January 1, 2013 to July 31, 2014. Daily estimates of evapotranspiration were calculated at 1 h intervals and summed for the daylight period.

Vegetation data

The average plant height and leaf area index (*LAI*) of each community were measured monthly by vegetation sampling and the LAI-2200 Plant Canopy Analyzer (LI-COR, Lincoln, Nebraska, USA), respectively (Figure 3). When the land was flooded, vegetation data measured in the corresponding period in 2011 were used instead. Since vegetation coverage was usually at its maximum during this period (July–August), the vegetation data (e.g., *LAI*) in 2011 was considered to be approximately the same as those in the next year.

Distribution of root length density was investigated in August 2013 when roots were fully developed. During the sampling time, the site was exposed and the groundwater depth in both vegetation communities was greater than

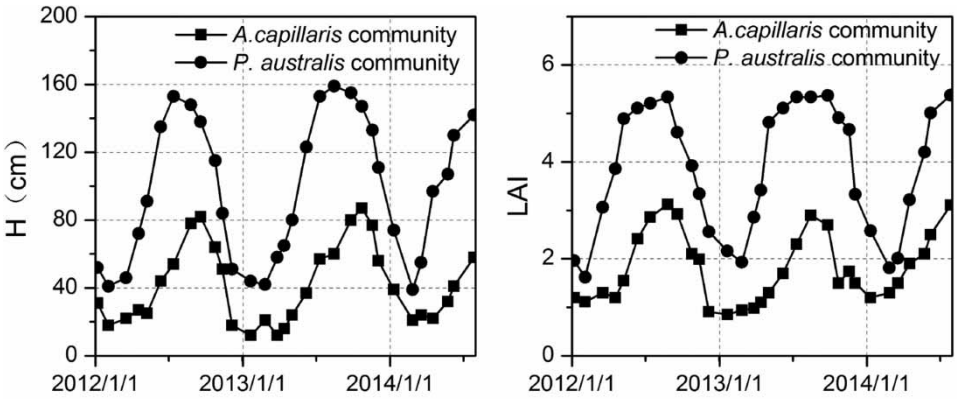

Figure 3 | Variations in average plant height (*H*) and *LAI* in the *A. capillaris* and *P. australis* communities.

2 m (Figure 2). Soil samples of 10 cm × 10 cm × 10 cm were excavated to a depth of 1 m until no obvious roots were discovered, and then carefully washed in 0.05 mm mesh screens to obtain all roots. The length of active roots (diameter <2 mm) at each soil layer was measured by a root scanner (WinRHIZO 2008, Canada).

Soil texture data

Soil samples were taken from the ground surface down to 160 cm depth in each community using a soil auger. Well construction revealed that soils deeper than 160 cm were silt and thus were treated as homogenous. Soil mechanical composition and bulk density were analyzed in the laboratory and are summarized in Table 1.

Conceptual model and water balance equation

As the water table gradient in our study site was less than 0.002 (Xu *et al.* 2014), lateral recharge was negligible and soil water movement occurred mainly through vertical exchange. Consequently, the conceptual models of *A. capillaris* and *P. australis* communities were generalized as a one-dimensional vertical groundwater–soil–plant–atmosphere continuum (Figure 4). The top boundary was selected at the soil surface. The bottom boundary was selected at the water table. The soil profile was classified into four layers in the *A. capillaris* community and three layers in the *P. australis* community based on a soil texture investigation (Table 1). The root zones of the *A. capillaris* and *P. australis* communities were generalized as 0–100 and 0–80 cm depth, respectively (see details in the section 'Root distribution'). The water balance of the root zone was expressed as:

$$(P - I - S_r) + G - D - E_a - T_a = \Delta W \quad (1)$$

where P is precipitation (mm), I is vegetation interception (mm), S_r is surface runoff (mm), G is groundwater upward fluxes to the root zone (mm), D is deep drainage (mm), E_a is actual soil evaporation (mm), T_a is actual plants' transpiration (mm), and ΔW is the changes of the root zone soil water

Table 1 | Measured soil texture composition and bulk density data

Community	Soil layer	Soil depth (cm)	Sand (%)	Silt (%)	Clay (%)	Bulk density (g/cm^3)	Soil texture
A. capillaris community	1	0–20	92.8	6.2	1.0	1.33	Sand
	2	20–80	91.2	7.8	1.0	1.26	
	3	80–120	84.2	9.6	6.2	1.35	
	4	120–160	54.2	36.4	10.4	1.37	Sandy silt
P. australis community	1	0–20	13.6	76.0	11.4	1.35	Silt
	2	20–80	23.1	64.3	12.5	1.24	
	3	80–160	17.7	68.4	13.9	1.40	

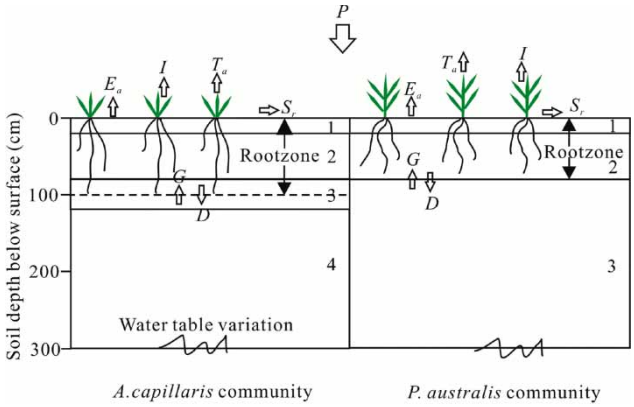

Figure 4 | Conceptual models of the *A. capillaris* and *P. australis* communities (*P*, precipitation; *I*, vegetation interception; S_r, surface runoff; T_a, actual plant transpiration; E_a, actual soil evaporation; *G*, groundwater upward flux to the root zone; *D*, deep drainage of root zone soil water. The meanings of these variables are the same henceforth. Arrows represent water flux direction, and the numbers represent different soil layers as in Table 1).

storage (mm). The rainfall infiltration through the soil surface (R_{in}, mm) was expressed as:

$$R_{in} = P - I - S_r \tag{2}$$

Model setup

HYDRUS-1D model description

Soil water flow was described by Richard's equation (Šimůnek *et al.* 2008):

$$\frac{\partial \theta}{\partial t} = \frac{\partial}{\partial z}\left[K(\theta)\left(\frac{\partial h}{\partial z} + 1\right)\right] - S(z, t) \tag{3}$$

where θ is the volumetric soil moisture ($cm^3\ cm^{-3}$), $K(\theta)$ is the unsaturated hydraulic conductivity (cm d^{-1}), t is the time (d), h is the pressure head (cm), z is the vertical coordinate (positive upward) (cm), $S(z, t)$ is the sink term ($cm^3\ cm^{-3}\ d^{-1}$), which represents the water uptake by roots.

The soil hydraulic conductivity properties were modeled by the van Genuchten model (van Genuchten 1980) as follows:

$$\theta(h) = \begin{cases} \theta_r + \dfrac{\theta_s - \theta_r}{\left[1 + |\alpha h|^n\right]^m} & h < 0 \\ \theta_s & h \geq 0 \end{cases} \tag{4}$$

$$K(\theta) = K_s S_e^{1/2}\left[1 - (1 - S_e^{1/m})^m\right]^2 \tag{5}$$

$$S_e = \frac{\theta(h) - \theta_r}{\theta_s - \theta_r} \tag{6}$$

where θ_r and θ_s are the residual and saturated soil moisture, respectively ($cm^3\ cm^{-3}$), K_s is the saturated hydraulic conductivity (cm d^{-1}), α is the reciprocal of air entry value (cm^{-1}), n is a pore size distribution parameter (–), $m = 1 - 1/n$, l is a pore connectivity parameter, with a value of 0.5 for common assumption, and S_e is the effective saturation ($cm^3\ cm^{-3}$).

The root water uptake term was expressed by the following equation (Skaggs *et al.* 2006b):

$$S(z, t) = \alpha(h) r(z) T_p \tag{7}$$

where T_p is the potential transpiration rate (cm d^{-1}), $r(z)$ is the normalized root length distribution function (cm^{-1}), and $\alpha(h)$ is a dimensionless stress response function ($0 \leq \alpha \leq 1$) that describes the water uptake reduction due to soil moisture deficit. $\alpha(h)$ was described by the S-shaped model (van Genuchten 1987):

$$\alpha(h) = \frac{1}{1 + (h/h_{50})^p} \tag{8}$$

where h_{50} is the pressure head (cm) at which potential transpiration is reduced by 50% and P is a constant that determines the steepness of transpiration decreasing along with an increase in the pressure head. Introduced by van Genuchten (1987), Equation (8) does not consider the water uptake reduction caused by hypoxia under saturated soil, and this seems justifiable for wetland plants with abundant aerenchyma.

Boundary and initial condition

The upper boundary was specified as the 'atmospheric' boundary condition and defined by rainfall infiltration and evapotranspiration. Potential evapotranspiration (ET_p) was first calculated by the FAO Penman–Monteith equation using meteorological data (Allen *et al.* 1998), including:

solar radiation, humidity, wind speed, maximum and minimum air temperature, sunshine hours, as well as crop characteristics, such as average plant height, the *LAI*, and surface albedo. Potential evaporation (E_p) and transpiration (T_p) were then calculated according to the Beer's law as in Equation (9) (Ritchie 1972). The E_a and T_a were finally determined based on simulated soil moisture conditions:

$$T_p = ET_p(1 - e^{-k.LAI})$$
$$E_p = ET_p e^{-k.LAI} \quad (9)$$

where k represents the radiation extinction coefficient and is assigned a value of 0.39, following Ritchie (1972) and Feddes *et al.* (1978).

In order to simulate water movement in the saturated–unsaturated zone, the lower boundary was selected below the water table level in the low stage period, at 10 and 8 m, respectively, in the *A. capillaris* and *P. australis* communities. The boundary was specified as a time-varying pressure head boundary and described by WTD measurements. The initial soil moisture profile was specified based on linear interpolation between soil moisture measured at January 1, 2012 and the saturated soil moisture below water level.

Root distribution

In the *A. capillaris* community, root length data showed that 51% of the active root length was distributed in the 0–20 cm soil layers, 33% in the 20–60 cm, and 16% in the 60–100 cm layers. In the *P. australis* community, 51% of the active root length was distributed in the 0–10 cm soil layers, 41% in the 10–40 cm, and 8% in the 40–80 cm layers. Then, the root length density distribution was modeled with the following normalized functions:

$$r(z)|_{A.capillaris} = \begin{cases} 82.2/L_R & 0 \le z \le 20\text{cm} \\ 26.6/L_R & 20 < z \le 60\text{cm} \\ 12.9/L_R & 60 < z \le 100\text{cm} \end{cases} \quad (10)$$

$$r(z)|_{P.australis} = \begin{cases} 470/L_R & 0 \le z \le 10\text{cm} \\ 126/L_R & 10 < z \le 40\text{cm} \\ 18.4/L_R & 40 < z \le 80\text{cm} \end{cases} \quad (11)$$

where $z = 0$ cm is the soil surface, $z = 100$ and 80 cm are the maximum rooting depths in the *A. capillaris* and *P. australis* communities, respectively, and L_R is the measured total length of roots, which equals to 3,222 and 6,217 cm in the *A. capillaris* and *P. australis* communities, respectively.

Model calibration and assessment

The model was calibrated and validated by comparing the simulated and field observed soil moisture at different depths. The simulated evapotranspiration in the *A. capillaris* community was also compared with the evapotranspiration estimated by the BREB method. Agreement between simulated and observed values was quantitatively assessed by Pearson's correlation coefficient (R), root mean square deviation ($RMSE$), and relative error (RE) using the following equations:

$$RMSE = \sqrt{\frac{1}{N}\sum_{i=1}^{N}(S_i - O_i)^2} \quad (12)$$

$$RE = \frac{\sum_{i=1}^{N} S_i}{\sum_{i=1}^{N} O_i - 1} \quad (13)$$

$$R = \frac{\sum_{i=1}^{N}(S_i - \overline{S})(O_i - \overline{O})}{\sqrt{\sum_{i=1}^{N}(S_i - \overline{S})^2 \cdot \sum_{i=1}^{N}(O_i - \overline{O})^2}} \quad (14)$$

where N is the number of data, S_i is the simulated value, O_i is the observed value, and $\overline{S}$ and $\overline{O}$ are the average values of the simulated and observed data, respectively.

RESULTS

Model calibration and validation

The calibration period was from January 1, 2012 to May 31, 2013, and the validation period was from June 1, 2013 to July 30, 2014. The simulated period included both wet and dry phases, allowing us to fit the model at a wide range of

soil water conditions. Thus, the calibrated model can reproduce a soil–water environment that more accurately reflects actual field conditions. Moreover, when the land was flooded from May 17, 2012 to August 31, 2012, the soil profile was saturated and vegetation transpiration and evaporation were both assigned at the potential rate.

Model parameters

The initial soil hydraulic parameters, θ_r, θ_s, α, n, and K_s, were estimated by inputting the soil bulk density and percentage of sand, silt, and clay (Table 1) into the Rosetta pedotransfer function model (Schaap *et al.* 2001). The Marquardt–Levenberg inverse algorithm, incorporated in the HYDRUS-1D model, was subsequently used to optimize these parameters using field-measured data (Marquardt 1963). The calibrated soil hydraulic parameters are shown in Table 2.

The parameter values of h_{50} and P in the S-shaped model ranged from −950 to −5,000 cm and 1.5 to 3, respectively, for different plants and soil types, as reported by previous studies (Skaggs *et al.* 2006a; Zhu *et al.* 2009). In the *A. capillaris* community, the soil texture in the root zone was mainly sand. Under this coarse soil, soil moisture usually decreased quickly. Consequently, relatively higher values of −950 cm and 3 were separately assigned to h_{50} and P for the *A. capillaris* community to represent a steep curve in the soil moisture drainage process. In addition, the h_{50} and P for the *P. australis* community were assigned values of −2,456 cm and 3, respectively, which were similar to the experimental results of Xie *et al.* (2011) for a *P. australis* community in a Yellow River delta wetland. In the calibration period, our results showed that simulated soil moisture varied slightly when these two parameters changed among the reported values. This agreed with the findings of Zhu *et al.* (2009) and Xie *et al.* (2011). Thus, the values of h_{50} and P in this study were not further calibrated.

Table 2 | Calibrated soil hydraulic parameters in *A. capillaris* and *P. australis* communities

Vegetation community	Soil depth (cm)	θ_r ($cm^3\ cm^{-3}$)	θ_s ($cm^3\ cm^{-3}$)	α (cm^{-1})	n (−)	K_s ($cm\ d^{-1}$)
A. capillaris community	0–20	0.05	0.47	0.031	2.31	277
	20–80	0.04	0.49	0.036	2.11	248
	80–120	0.05	0.48	0.008	3.46	183
	120–1,000	0.04	0.48	0.022	1.34	75
P. australis community	0–20	0.06	0.46	0.008	1.08	102
	20–80	0.05	0.46	0.005	1.14	80
	80–800	0.06	0.46	0.009	1.08	45

Calibration results

The simulated and observed soil moisture at 10, 50, and 100 cm depths in the *A. capillaris* and *P. australis* communities for both calibration and validation periods are shown in Figure 5. The simulated soil moisture displayed similar variation tendencies as the observed data by visual comparison. The differences between simulated and observed values were partly due to model uncertainty, soil spatial heterogeneity, and observation errors, which are inevitable in field conditions and model setup. The observed soil moisture remained low from January 1 to June 30, 2012 while the simulated soil water content increased with rainfall. The reason for this discrepancy was presumably due to the influences of initial field observation and the model warm-up period, which were more or less non-existent after a certain period of time when the system operated stably. Overall, the HYDRUS-1D model was capable of simulating the seasonal variations of field soil water content. For the *A. capillaris* community, the *RMSE* of soil moisture ranged from 0.03 to 0.07 $cm^3\ cm^{-3}$ in both calibration and validation periods, the *RE* values varied from −0.00 to 0.16, and the *R* values were within 0.85–0.96 (Table 3). For the *P. australis* community, the *RMSE* ranged from 0.03 to 0.04 $cm^3\ cm^{-3}$, the *RE* varied from −0.02 to 0.03, and the *R* values were within 0.81–0.92. The simulations were in good agreement with the measurements.

Simulated actual evapotranspiration in the *A. capillaris* community also showed similar variations and amounts as the BREB estimated evapotranspiration (Figure 6). The *RMSE* of evapotranspiration in the *A. capillaris* community varied from 0.50 to 1.01 mm/d, *RE* ranged from −0.08 to −0.10, and *R* values were within 0.73–0.89 (Table 3). Although the simulated results were satisfactory, the model somewhat overestimated the evapotranspiration in June–August, 2013. This is possibly due to differences in the measuring principles of the BREB method and the model simulation. The BREB estimated evapotranspiration is mainly based on energy balance and represents the

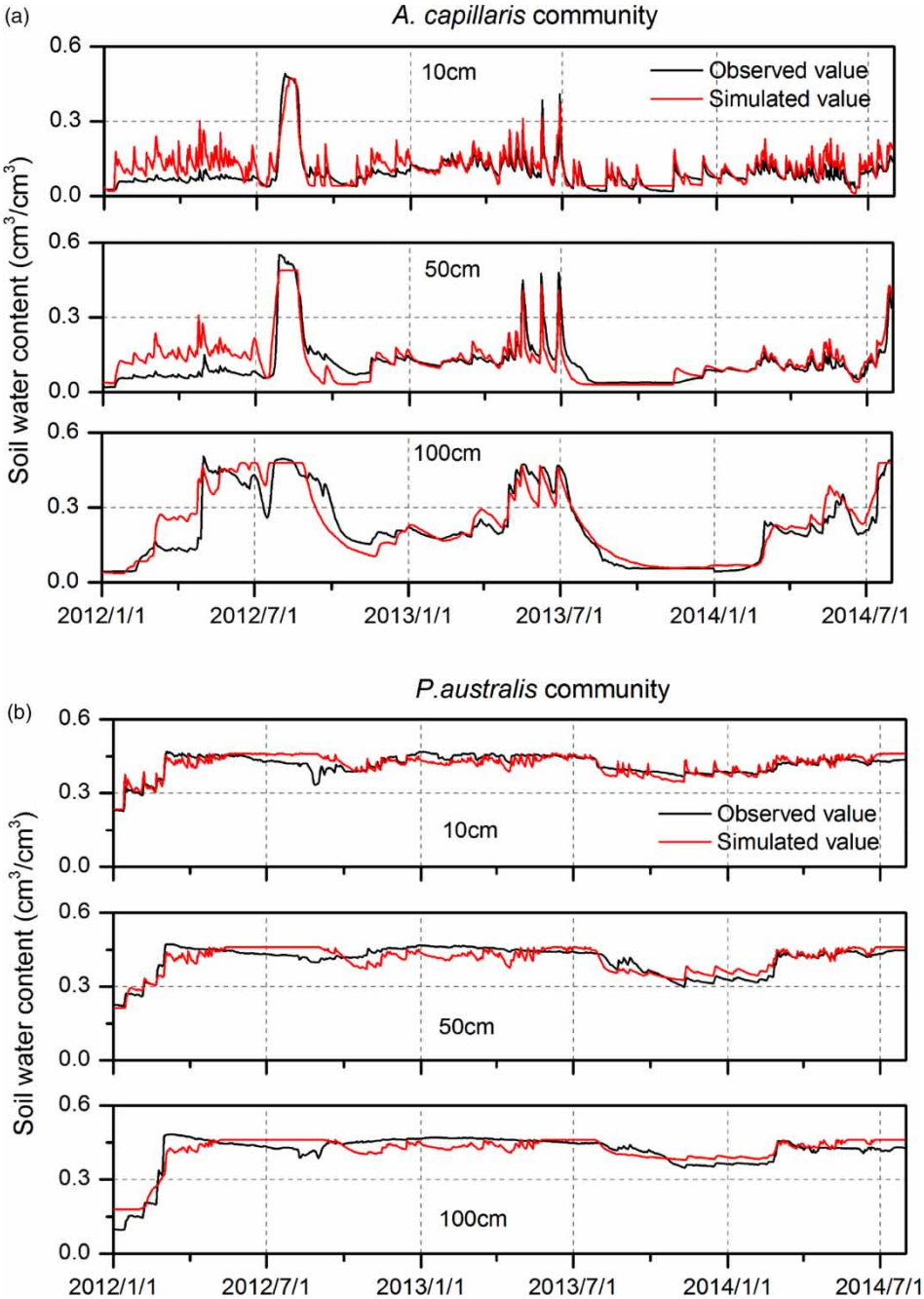

Figure 5 | Comparison of observed and simulated soil moisture at three depths for calibration (January 1, 2012–May 31, 2013) and validation (June 1, 2013–July 30, 2014) periods in the *A. capillaris* (a) and *P. australis* (b) communities.

average situation over a wide area for a hundred meters, while the simulated evapotranspiration is more representative for a specific location of the field (Perez *et al.* 1999; Qiang *et al.* 2009). Moreover, the application of the BREB method requires uniform underlying surface and horizontal advection to be negligible (Wang 2003). That is not easy to satisfy during July–August in the flooding seasons when most of the wetland is flooded, because the thermal contrast between the land and water area in summer usually leads to obvious horizontal advection (Figuerola & Berliner 2006).

Table 3 | Assessment of the observed and simulated soil moisture and evapotranspiration in calibration and validation periods

			Calibration			Validation		
Vegetation	**Items**	**Soil depth**	***RMSE***	***RE***	***R***	***RMSE***	***RE***	***R***
A. capillaris community	θ	10 cm	0.04	0.10	0.91	0.03	0.16	0.85
		50 cm	0.05	−0.00	0.88	0.03	−0.00	0.88
		100 cm	0.07	0.02	0.87	0.04	0.08	0.96
	ET_a	–	0.50	−0.10	0.89	1.01	−0.08	0.73
P. australis community	θ	10 cm	0.03	−0.00	0.82	0.02	0.00	0.90
		50 cm	0.03	−0.02	0.84	0.02	0.03	0.91
		100 cm	0.04	−0.02	0.92	0.02	0.03	0.81

Note: The unit for *RMSE* for θ is $cm^3\ cm^{-3}$ and for ET_a is mm d^{-1}.

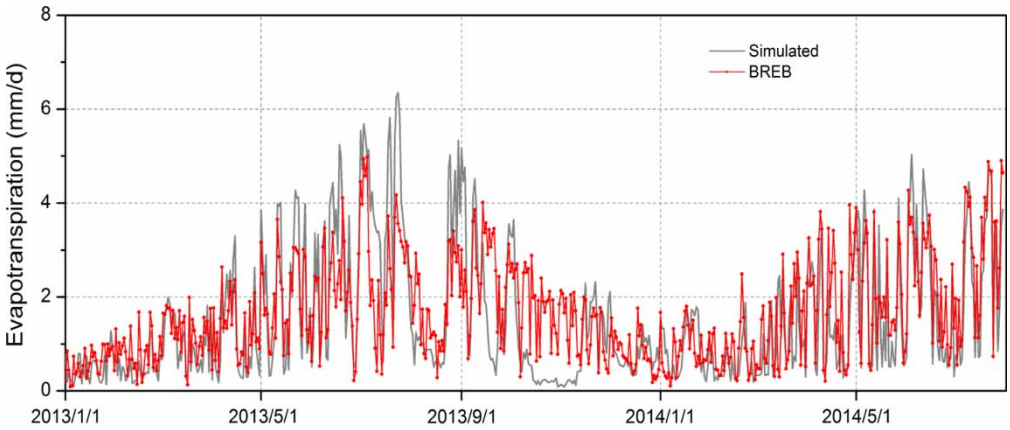

Figure 6 | Comparison of simulated evapotranspiration and evapotranspiration estimated by BREB in the *A. capillaris* community for calibration (January 1, 2013–May 31, 2013) and validation (June 1, 2013–July 30, 2014) periods.

In addition, the simulated evapotranspiration was reduced drastically (according to Equation (5)) in October 2013 as soil moisture decreased to the residual soil moisture, whereas the evapotranspiration estimated by BREB was not reduced. This difference may be because dew formation occurs frequently in autumn at the study site. The contribution of dew to evapotranspiration in early morning was included in the BREB measurements, but was not able to be considered in the HYDRUS-1D model. However, since this paper primarily concentrates on vegetation transpiration, we considered the simulated results to be reasonable. These goodness-of-fit values indicated satisfactory agreement between simulated values and field measurements, and demonstrated the acceptable accuracy of model simulations.

Vegetation transpiration and groundwater contribution in different hydrological years

Temporal variation of water fluxes

Figure 7 presents the monthly variations of the simulated water fluxes in the *A. capillaris* and *P. australis* communities. Two different stages throughout the annual scale can be observed according to the variation of evapotranspiration and rainfall infiltration.

In the initial growth stage from April to June, the actual evapotranspiration of the *A. capillaris* and *P. australis* communities totaled 157–163 and 328–338 mm, respectively, and were equal to the potential level (Table 4). This period is also the wet season in Poyang Lake, and the rainfall

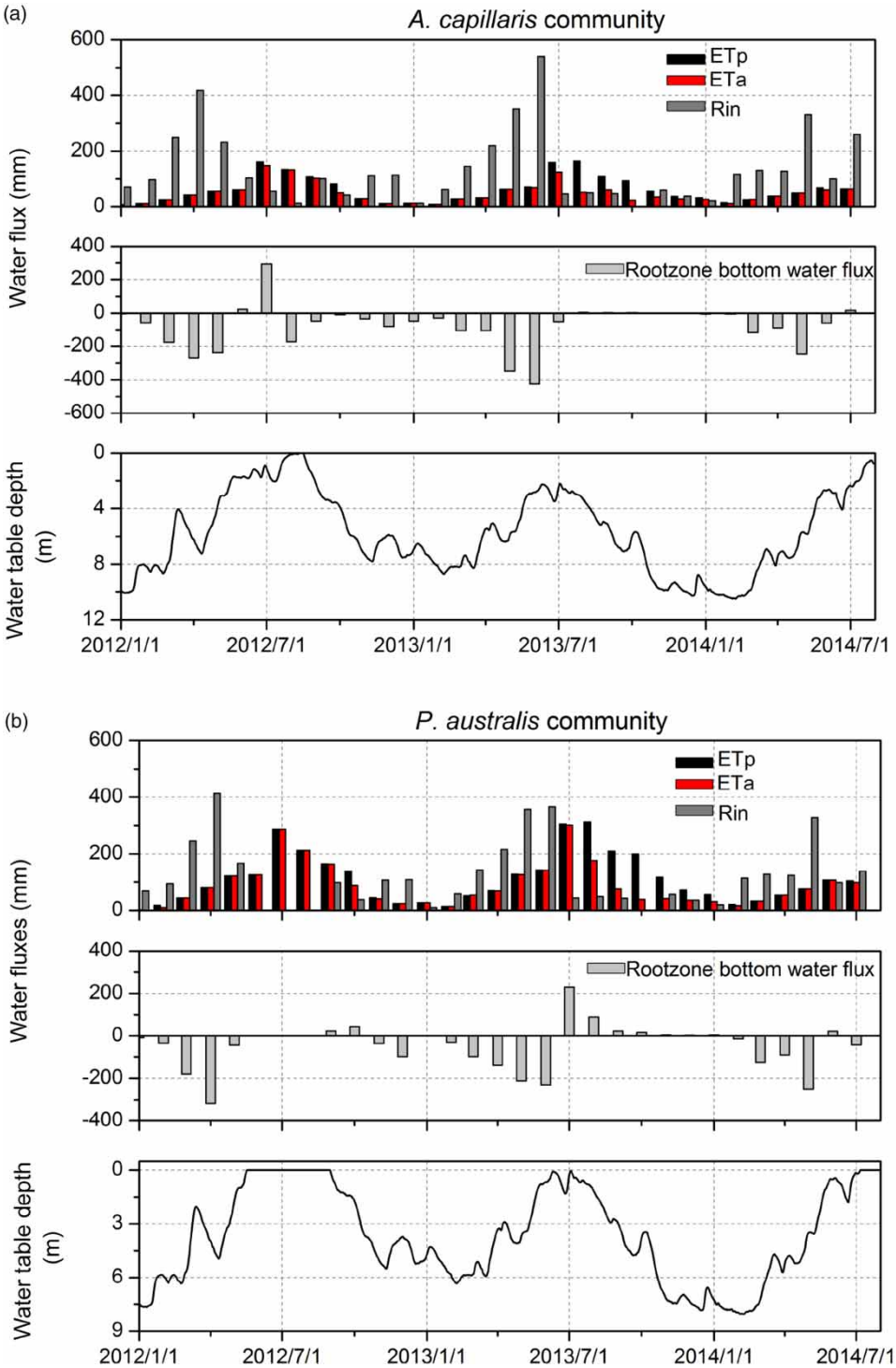

Figure 7 | Monthly variations of the simulated water fluxes across the top boundary and the lower root zone in *A. capillaris* (a) and *P. australis* (b) communities.

infiltration amounted to 752–1,110 mm, accounting for approximately 55% of the annual amount. It is obvious that in this stage, rainfall can satisfy the evapotranspiration water demand and water was not a limiting factor for vegetation growth. With large amounts of rainfall infiltrating, the root zone bottom was mainly experiencing downward

Table 4 | Water balance of the *A. capillaris* and *P. australis* communities in initial (April–June) and main (July–October) growth stages in high (2012) and low (2013) water table years

Community	Hydrological year	Stage	T_p	T_a	E_a	ET_a	R_{in}	G	D	ΔW	AE	T_a/T_p
A. capillaris	High	initial	96	96	61	157	752	74	557	107	−5	1.00
		main	349	334	96	430	209	439	375	−161	−4	0.96
	Low	initial	90	90	73	163	1,110	0	877	66	−4	1.00
		main	367	203	54	257	143	13	51	−154	−2	0.55
P. australis	High	initial	125	125	17	142	510	96	457	10	3	1.00
			173[a]	173[a]	13[a]	186[a]	–	–	–	–	–	
		main	458[b]	458[b]	43[b]	501[b]	–	–	–	–	–	0.92
			277	219	39	258	136	161	92	−50	3	
	Low	initial	307	307	31	338	937	182	762	15	−4	1.00
		main	943	510	89	599	137	401	39	−95	5	0.54

Note: T_p, T_a, E_a, R_{in}, G, and D, in mm; ΔW, changes of root zone soil water storage, in mm; AE, absolute error, in mm. Data marked with superscripts 'a' and 'b' represent water flux calculated in the flood period from May 16 to June 30, 2012 and from July 1 to August 31, 2012, respectively. E_a represents soil/water evaporation when the land was exposed/flooded, respectively.

soil water movement (Figure 7). The cumulative amount of percolation in the *A. capillaris* and *P. australis* communities comprised about 74%–90% of the rainfall infiltration.

In the main growth stage from July to October, the actual evapotranspiration amounts of the *A. capillaris* and *P. australis* communities increased significantly to 257–430 and 599–759 mm, respectively. However, rainfall infiltration decreased sharply to less than 210 mm, which was much lower than evapotranspiration. During this period, upward water movement across the root zone bottom existed under the high water table condition (Figure 7). This indicates that rainfall in this stage cannot satisfy plant water demand, and vegetation transpiration must depend on the groundwater contribution.

Vegetation transpiration

According to variation in the depth of the water table, 2012 and 2013 represented high and low water table years, respectively (Figure 2(b)). Significant differences in vegetation transpiration in the main growth stage were detected between the two different hydrological years (Figure 7, Table 4). In the high water table year, the actual transpiration of *A. capillaris* and *P. australis* communities in the main growth stage totaled 334 and 677 mm, respectively, accounting for 96% and 92% of the potential transpiration totals. However, in the low water table year, the actual transpiration in this period added up to 203 and 510 mm, respectively, only accounting for approximately 55% of the potential transpiration totals due to there being insufficient water to support potential water uptake (according to Equation (7)). This revealed that in low water table conditions, vegetation transpiration in the main growth stage was constrained by the water deficit.

The time course of the T_a/T_p ratio in the main growth stage also showed substantial differences between the high and low water table years (Figure 8). In the high water table year, the ratio remained constantly around 1 during July–September and only decreased in October (Figure 8(a)). However, in the low water table year, the ratio decreased significantly in early August and even fell below 0.4 for a relatively long period during August–October (Figure 8(b)). This indicated that in high water table years, vegetation transpiration was only affected by a slight lack of water in October; whereas in low water table years, it was severely constrained by a water deficit during August–October. Moreover, considering that the T_a/T_p ratio of the *A. capillaris* community was higher than that of the *P. australis* community, we concluded that the *P. australis* community may suffer more severe water stress than the *A. capillaris* community.

Groundwater contribution

Two water sources contribute to vegetation transpiration when the wetlands are exposed: rainfall infiltration and upward fluxes of groundwater. By comparing the totals, we found that groundwater plays an important role in vegetation transpiration in the main growth stage.

In the main growth stage of the high water table year, the WTD in the *A. capillaris* community varied from 0 to

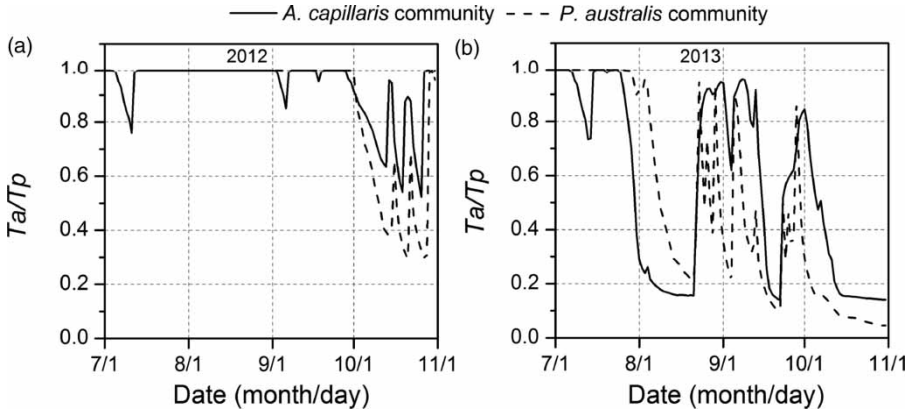

Figure 8 | T_a/T_p ratio of the *A. capillaris* and *P. australis* communities in the main growth stage of high ((a) 2012) and low ((b) 2013) water table years.

7.2 m, with a mean value of 2.6 m (Figure 2(b)), and a cumulative 439 mm of groundwater moved up into the root zone (Table 4). The groundwater contribution was able to satisfy the entire amount of water lost to transpiration (334 mm) in the *A. capillaris* community. Whereas, in the main growth stage of the low water table year, WTD varied within 2.2–9.6 m, with a mean value of 5.3 m, and the amount of groundwater supplied to the root zone was only 13 mm, which accounted for merely 6% of the transpiration totals (203 mm). This indicates that WTD directly determines the groundwater contribution to root zone soil moisture and affects the transpiration water consumption of the *A. capillaris* community.

In the *P. australis* community, a direct groundwater contribution to root zone soil moisture existed in the main growth stage when the land was exposed (Figure 7(b)). In the high water table year, the land was exposed from September, and the WTD ranged from 0 to 4.9 m with an average of 2.4 m during September–October (Figure 2(b)). The cumulative amount of groundwater moving upward into the root zone was 161 mm, which could account for a maximum of 74% of the water (219 mm) transpired by the *P. australis* community during September–October. However, in the low water table year, a mean water table of 3.0 m depth (varied within 0–7.1 m) in the main growth stage resulted in a groundwater contribution of 401 mm, which accounted for 79% of the transpiration totals (510 mm). These results indicated that most of the water transpired by the *P. australis* community in the main growth stage originated from groundwater when the wetland was exposed. In low water table years without inundation, groundwater recharge directly determined the available water for the *P. australis* community.

Effects of WTD on vegetation transpiration

Based on the validated HYDRUS-1D model, simulation scenarios with constant *WTD* from July to October ranging from 0.5 to 3 m in 0.5 m increments were performed to further evaluate the influence of WTD on vegetation transpiration in the main growth stage. To make the results more representative of average meteorological conditions, scenario simulations were driven by daily averaged meteorological observations from 1955 to 2011 at the Duchang hydrological station (18 km from the study site). Soil texture and plant characteristics were the same as those used in the validated model.

Transpiration variation under different WTD

The simulated scenarios of $WTD = 0.5$ and 1 m had the highest transpiration, with totals of 376 and 926 mm for the *A. capillaris* and *P. australis* communities, respectively. The water stress T_a/T_p ratio of the *A. capillaris* and *P. australis* communities was equal to 1 for both cases (Table 5). This suggested that when *WTD* was within 1 m, soil moisture was sufficient to sustain plants using water at the potential rate and transpiration was completely controlled by atmospheric demand.

Table 5 | Simulated cumulative transpiration and upward fluxes of groundwater across root zone bottom in the main growth stage (July–October) for different WTD scenarios

	A. capillaris community				*P. australis* community			
WTD (m)	T_a (mm)	G (mm)	G/T_a (–)	T_a/T_p (–)	T_a (mm)	G (mm)	G/T_a (–)	T_a/T_p (–)
0.5	376	213	0.57	1.00	926	715	0.77	1.00
1.0	376	209	0.56	1.00	925	711	0.77	1.00
1.5	328	135	0.44	0.87	782	554	0.71	0.84
2.0	280	69	0.25	0.74	515	266	0.52	0.56
2.5	261	34	0.13	0.69	407	150	0.37	0.44
3.0	254	17	0.07	0.68	364	102	0.28	0.39

Vegetation transpiration and the *Ta/Tp* ratio both decreased significantly with increasing *WTD* larger than 1 m, indicating that plant transpiration becomes limited by intensified water deficit. When the *WTD* was increased from 1 to 3 m, transpiration decreased to approximately 254 mm for the *A. capillaris* community and 364 mm for the *P. australis* community.

Relationship between groundwater contribution ratio and WTD

The simulated cumulative upward fluxes of groundwater to root zone soil moisture also decreased with increasing *WTD* (Table 5). With *WTD* within 1 m, approximately 209–213 and 711–715 mm of groundwater moved into the root zone of the *A. capillaris* and *P. australis* communities, respectively. Increasing the *WTD* from 1 to 2 m reduced the upward fluxes of groundwater to the *A. capillaris* and *P. australis* communities to 69 and 266 mm, respectively. When the *WTD* was further increased to 3 m, it was decreased by 92% and 86%, respectively.

The ratio of groundwater contributions (G) to vegetation transpiration (T_a) at different depths is shown in Table 5. It decreased with increasing *WTD*, which is in accordance with previous results (Luo & Sophocleous 2010; Xie *et al.* 2011). Under long-term annual average meteorological conditions, groundwater upward flow contributed as much as 56% and 77% of the vegetation transpiration of the *A. capillaris* and *P. australis* communities at *WTD* within 1 m, respectively. When the water table was lowered to 3 m depth, the groundwater contributions to the transpiration of the *A. capillaris* and *P. australis* communities decreased to approximately 7% and 28%, respectively.

Regression analysis was used to determine the relationship between the contribution of groundwater to vegetation transpiration (G/T_a) and *WTD* in the main growth stage. The equations are shown as follows:

$$\frac{G}{T_a} = 0.79 - 0.25WTD,$$
$$R^2 = 0.98,\ P < 0.001, \text{ for } A.\ capillaris \text{ community} \quad (15)$$

$$\frac{G}{T_a} = 1.05 - 0.26WTD,$$
$$R^2 = 0.98,\ P < 0.001, \text{ for } P.\ australis \text{ community} \quad (16)$$

Similar linear relationships were also reported by Grismer & Gates (1988) and Sepaskhah *et al.* (2003); Sepaskhah & Karimi-Goghari (2005). According to the similar slopes of Equations (15) and (16), we know that the contribution of groundwater to vegetation transpiration decreased by approximately 25% for every 1 m decline in the water table. In addition, the intercept for the *P. australis* community was higher than that for the *A. capillaris* community. This may indicate that groundwater plays a more important role in transpiration of the *P. australis* community than the *A. capillaris* community.

DISCUSSION

Water movement through the groundwater–soil–plant–atmosphere continuum is fundamental in the study of wetland eco-hydrological processes (Mazur *et al.* 2014). Numerical simulation has become an important method for water movement research. However, the complex wetland environment and limited monitoring methods made it still difficult to explore interface water transfer (Deng & Hu 2003; Xie *et al.* 2011). This study quantified the interfaces water flux dynamics in a typical river-connected lake wetland with large water level variations, and assessed the influence of WTD on vegetation transpiration. The results are helpful for a better understanding of the interactions of groundwater, soil

water, and vegetation, and may provide reasonable references for wetland conservation and management.

In this study, continuous field observations of meteorology, hydrology, soil, and vegetation were conducted at an experimental site. The HYDRUS-1D model was well calibrated by soil water content and evapotranspiration with reasonable accuracy (Table 3). It should be noted that the root zone bottom water fluxes data are not available in the study, thus further calibration may be necessary by using the measurements of a lysimeter. As well, the assumption of 1D vertical soil water movement was applied to the study area. This assumption may be regarded as valid for the following reasons. First, the water table gradient is less than 0.002 in the site, implying a weak lateral water movement. Second, the soil texture is mainly composed of sand without a clay course, and thus no obvious lateral subsurface runoff is generated. However, portions of clay components usually increase significantly at low regions near the main lake area (Liu *et al.* 2000). As such, it would be more reasonable to extend the current model to a 2D vertical simulation to account for lateral water movement. Nonetheless, the present model is adequate as a first attempt to achieve the objectives of this study.

In river riparian and seasonally flooded wetlands, vegetation usually shows a zonal distribution pattern along the WTD gradient (Dwire *et al.* 2006). Many studies have indicated that plant composition and community construction are controlled by their ability to cope with the flooding that characterizes hypoxia environments (Ferreira 2000; Leyer 2005). Indeed, most wetland plants can reduce damage from low oxygen stress by developing aerenchyma and morphology adjustments (Coops *et al.* 1996; Qin *et al.* 2013). However, wetlands usually alternate between flooding and drought, especially under large variations in the depth of the water table, and consequently, plants typically suffer periodic drought stress (Sommer *et al.* 2003; Hammersmark *et al.* 2009; Xie *et al.* 2011; Li *et al.* 2013). Our results supported this point, finding serious water deficit for transpiration of the *A. capillaris* and *P. australis* communities during August–October in low water level years. As the water tables declines, seasonally flooded wetlands usually face a reduced water supply, which constrains plant water absorption. Some studies have suggested that flood-tolerant wetland plants usually have a low tolerance to drought, since a trade-off exists in species between tolerance to flood and tolerance to drought (Luo *et al.* 2008; Li *et al.* 2013). Clearly, drought is another severe stress influencing wetland plant growth, and it might impose more harm to plants than flooding.

In the Poyang Lake wetland, severe droughts have occurred frequently during the 21st century, particularly serious autumn dryness (Jiao 2009; Zhang *et al.* 2012b). Lake water levels from September to November in the 2000s were the lowest in nearly 60 years, with the minimum level even breaking the record low minimum value (Zhang *et al.* 2014). Consequently, the upland wetland habitats are exposed earlier and longer than normal under the decreasing water levels (Hu *et al.* 2010; Gan *et al.* 2011; Lai *et al.* 2012). Our results demonstrated that the low water table (e.g., in 2013) caused severe water stress for upland wetland vegetation transpiration during August–October. This might be one of the primary reasons for the upland wetland vegetation degradation and expansion towards the lake. Some studies have implied that the autumn dryness in the Poyang Lake wetland may be worsened in the future due to less catchment discharge in dry seasons and the construction of more dams on the upper reaches of the Yangtze River (Min & Min 2010; Ye *et al.* 2011; Zhang *et al.* 2014). This might cause the wetland water table to decline further and exacerbate the water shortages affecting vegetation transpiration in autumn. Consequently, interspecific competition for scare water may enhance among plants when the wetland is exposed. Over the long term, drought-tolerant plants might become dominant due to their stronger water competitiveness compared to flood-tolerant plants. Ultimately, the severe water stress is likely to accelerate the positive succession of Poyang Lake wetland vegetation.

CONCLUSION

In floodplain wetlands, understanding the effect of WTD on vegetation transpiration is important for revealing the interactions between soil water and vegetation. In this study, HYDRUS-1D models were used to explore the changes in groundwater contribution and vegetation transpiration for two vegetation communities under different WTD conditions in the Poyang Lake wetlands. The models were

calibrated using field-measured soil moisture, and good agreements were achieved. The simulated results will be vitally helpful in predictions of the potential impacts of water table variation on wetland vegetation ecosystems under the background of climate change. The main conclusions are as follows:

1. In the initial growth stage (April–June), rainfall was higher than evapotranspiration, while in the main growth stage (July–October), rainfall could not satisfy plant water demand and transpiration was influenced by WTD. In the high water table year, vegetation transpiration comprised over 90% of the potential transpiration values; whereas in the low water table year, the transpiration totals accounted for only 55% of the potential transpiration totals, indicating severe water deficit. In the high water table year, upward fluxes of groundwater satisfied the transpiration water consumption of the *A. capillaris* community, while in the low water table year, it contributed merely 6% of the transpiration totals. In both years, groundwater contributed over 70% of the water transpired by the *P. australis* community in the main growth stage when the land was exposed.
2. Scenario simulations with constant WTDs in the main growth stage revealed significant decreases of vegetation transpiration with increasing WTD. When WTD was at 1 m, vegetation transpiration of the *A. capillaris* and *P. australis* communities could remain at potential levels, at which groundwater could contribute 56% and 77% of the transpiration totals, respectively. The ratio of groundwater contributions to vegetation transpiration decreased with WTD and could be described by linear equations for the *A. capillaris* and *P. australis* communities. Every 1 m decrease of water table resulted in approximately 25% reductions of the groundwater contribution ratio.

This study provides improved understanding of vertical water transportation in a groundwater–soil–plant–atmosphere system, exemplified in the Poyang Lake wetland. The results showed that WTD conditions significantly influenced vegetation transpiration. In addition, the findings of this study indicated that vegetation may also suffer periodic water stress in floodplain wetlands with large water level variation amplitudes. We recommend that further investigation of vegetation water use in humid regions should consider the influence of groundwater supply in dry seasons.

ACKNOWLEDGEMENTS

This study is funded by the National Natural Science Foundation of China (41371062), the National Basic Research Program of China (2012CB417003), and the Science Foundation of Nanjing Institute of Geography and Limnology, CAS (NIGLAS2012135001). We are also grateful to Mr Tan Zhiqiang, Miss Li Mengfan, and Miss Li Miao for assistance with field and laboratory work.

REFERENCES

Allen, R., Pereira, L. S., Raes, D. & Smith, M. 1998 *Crop evapotranspiration: guidelines for computing crop water requirements, FAO Irrigation and Drainage Paper 56*. Food and Agriculture Organization of the United Nations, Rome, Italy.

Baschuk, M. S., Koper, N., Wrubleski, D. A. & Goldsborough, G. 2012 Effects of water depth, cover and food resources on habitat use of marsh birds and waterfowl in boreal wetlands of Manitoba, Canada. *Waterbirds* **35** (1), 44–55.

Blanken, P. D. 2014 The effect of winter drought on evaporation from a high-elevation wetland. *J. Geophys. Res. Bio-Geosci.* **119** (7), 1354–1369.

Candela, L., Igel, W. V., Elorza, F. J. & Aronica, G. 2009 Impact assessment of combined climate and management scenarios on groundwater resources and associated wetland (Majorca, Spain). *J. Hydrol.* **376** (3–4), 510–527.

Chaves, M. M., Maroco, J. P. & Pereira, J. S. 2003 Understanding plant responses to drought–from genes to the whole plant. *Funct. Plant Biol.* **30** (3), 239–264.

Cooper, D. J., Sanderson, J. S., Stannard, D. I. & Groeneveld, D. P. 2006 Effects of long-term water table drawdown on evapotranspiration and vegetation in an arid region phreatophyte community. *J. Hydrol.* **325** (1–4), 21–34.

Coops, H., van den Brink, F. W. B. & van der Velde, G. 1996 Growth and morphological responses of four helophyte species in an experimental water-depth gradient. *Aquat. Bot.* **54** (1), 11–24.

Deng, W. & Hu, J. M. 2003 Development of wetland hydrology research and key scientific issues. *Wetland Sci.* **1** (1), 13–20 (in Chinese).

Deng, W., Pan, X. L. & Luan, Z. Q. 2003 Advances in wetland hydrology. *Adv. Water Sci.* **14** (4), 521–526 (in Chinese).

Dronova, I., Gong, P. & Wang, L. 2011 Object-based analysis and change detection of major wetland cover types and their classification uncertainty during the low water period at Poyang Lake, China. *Remote Sens. Environ.* **115** (12), 3220–3236.

Dwire, K. A., Kauffman, J. B. & Baham, J. E. 2006 Plant species distribution in relation to water-table depth and soil redox potential in Montane riparian meadows. *Wetlands* **26** (1), 131–146.

Fay, P. A. & Schultz, M. J. 2009 Germination, survival, and growth of grass and forb seedlings: effects of soil moisture variability. *Acta Oecol.* **35** (5), 679–684.

Feddes, R. A., Kowalik, P. J. & Zaradny, H. 1978 *Simulation of Field Water Use and Crop Yield*. John Wiley and Sons, New York, NY, USA.

Ferreira, L. V. 2000 Effects of flooding duration on species richness, floristic composition and forest structure in river margin habitat in Amazonian black water floodplain forests: implications for future design of protected areas. *Biodivers. Conserv.* **9** (1), 1–14.

Figuerola, P. I. & Berliner, P. R. 2006 Characteristics of the surface layer above a row crop in the presence of local advection. *Atmosfera* **19** (2), 75–108.

Gan, X. Y., Liu, C. L. & Huang, X. M. 2011 Study on the drought in Poyang Lake. *J. Anhui Agric. Sci.* **39** (24), 14676–14678 (in Chinese).

Gilliam, J. W. 1994 Riparian wetlands and water quality. *J. Environ. Qual.* **23** (5), 896–900.

Grismer, M. E. & Gates, T. K. 1988 Estimating saline water table contribution to crop water use. *Calif. Agric.* **42**, 23–24.

Hammersmark, C. T., Rains, M. C., Wickland, A. C. & Mount, J. F. 2009 Vegetation and water-table relationships in a hydrologically restored riparian meadow. *Wetlands* **29** (3), 785–797.

Hu, Z. P., Ge, G., Liu, C. L., Chen, F. S. & Li, S. 2010 Structure of Poyang lake wetland and plants ecosystem and influence of lake water level for the structure. *Res. Environ. Yangtze Basin* **19** (6), 597–605 (in Chinese).

Hurst, C. A., Thorburn, P. J., Lockington, D. & Bristow, K. L. 2004 Sugarcane water use from shallow water tables: implications for improving irrigation water use efficiency. *Agric. Water Manage.* **65** (1), 1–19.

Hussey, B. H. & Odum, W. E. 1992 Evapotranspiration in tidal marshes. *Estuaries* **15** (1), 59–67.

Jiao, L. 2009 Science news: scientists line up against dam that would alter protected wetlands. *Science* **326** (5952), 508–509.

Jimenez-Martinez, J., Skaggs, T. H., van Genuchten, M. T. & Candela, L. 2009 A root zone modelling approach to estimating groundwater recharge from irrigated areas. *J. Hydrol.* **367** (1–2), 138–149.

Johansen, O. M., Pedersen, M. L. & Jensen, J. B. 2011 Effect of groundwater abstraction on fen ecosystems. *J. Hydrol.* **402** (3–4), 357–366.

Kahlown, M. A., Ashraf, M. & Zia-ul-Haq 2005 Effect of shallow groundwater table on crop water requirements and crop yields. *Agric. Water Manage.* **76** (1), 24–35.

Lai, X. J., Jiang, J. H. & Huang, Q. 2012 Water storage effects of three gorges project on water regime of Poyang Lake. *J. Hydroelectricity Eng.* **31** (6), 132–136 (in Chinese).

Legesse, D., Vallet-Coulomb, C. & Gasse, F. 2004 Analysis of the hydrological response of a tropical terminal lake, Lake Abiyata (Main Ethiopian Rift Valley) to changes in climate and human activities. *Hydrol. Processes* **18** (3), 487–504.

Leyer, I. 2005 Predicting plant species responses to river regulation: the role of water level fluctuations. *J. Appl. Ecol.* **42** (2), 239–250.

Li, S. H., Zhou, D. M., Luan, Z. Q., Pan, Y. & Jiao, C. W. 2011 Quantitative simulation on soil moisture contents of two typical vegetation communities in Sanjiang Plain, China. *Chin. Geog. Sci.* **21** (6), 723–733.

Li, F., Qin, X. Y., Xie, Y. H., Chen, X. S., Hu, J. Y., Liu, Y. Y. & Hou, Z. Y. 2013 Physiological mechanisms for plant distribution pattern: responses to flooding and drought in three wetlands from Dongting Lake, China. *Limnology* **14** (1), 71–76.

Li, Y. L., Zhang, Q., Yao, J., Werner, A. D. & Li, X. H. 2014 Hydrodynamic and hydrological modeling of Poyang Lake-Catchment system in China. *J. Hydrol. Eng.* **19** (3), 607–616.

Liu, X. Z., Ye, J. X. & Ding, D. S. 2000 *Jiangxi Wetland. Department of Forestry in Jiangxi Province*. China Forestry Press, Beijing, China (in Chinese).

Lu, X. X., Yang, X. K. & Li, S. Y. 2011 Dam not sole cause of Chinese drought. *Nature* **475** (7355), 174.

Luo, Y. & Sophocleous, M. 2010 Seasonal groundwater contribution to crop-water use assessed with lysimeter observations and model simulations. *J. Hydrol.* **389** (3–4), 325–335.

Luo, W. B., Song, F. B. & Xie, Y. H. 2008 Trade-off between tolerance to drought and tolerance to flooding in three wetland plants. *Wetlands* **28** (3), 866–873.

Mansell, R. S., Bloom, S. A. & Sun, G. 2000 A model for wetland hydrology: description and validation. *Soil Sci.* **165** (5), 384–397.

Marquardt, D. W. 1963 An algorithm for least-squares estimation of nonlinear parameters. *SIAM. J. Appl. Math.* **11** (2), 431–441.

Mazur, M. L. C., Wiley, M. J. & Wilcox, D. A. 2014 Estimating evapotranspiration and groundwater flow from water-table fluctuations for a general wetland scenario. *Ecohydrology* **7** (2), 378–390.

Min, Q. & Min, D. 2010 Drought change characteristics and drought protection countermeasures for Poyang Lake Basin. *J. China. Hydrol.* **30** (1), 84–88 (in Chinese).

Mortsch, L. D. 1998 Assessing the impact of climate change on the Great Lakes shoreline wetlands. *Climatic Change* **40** (2), 391–416.

Mueller, L., Behrendt, A., Schalitz, G. & Schindler, U. 2005 Above ground biomass and water use efficiency of crops at shallow water tables in a temperate climate. *Agric. Water Manage.* **75** (2), 117–136.

Muneepeerakul, C. P., Miralles-Wilhelm, F., Tamea, S., Rinaldo, A. & Rodriguez-Iturbe, I. 2008 Coupled hydrologic and

vegetation dynamics in wetland ecosystems. *Water Resour. Res.* **44** (7), W07421.

Pagter, M., Bragato, C. & Brix, H. 2005 Tolerance and physiological responses of *Phragmites australis* to water deficit. *Aquat. Bot.* **25** (3), 520–530.

Pattern, D. T., Rouse, L. & Stromberg, J. C. 2008 Isolated spring wetlands in the Great Basin and Mojave Deserts, USA, potential response of vegetation to groundwater withdrawal. *Environ. Manage.* **41** (3), 398–413.

Perez, P. J., Castellvi, F., Ibanez, M. & Rosell, J. I. 1999 Assessment of reliability of Bowen ratio method for partitioning fluxes. *Agric. For. Meteorol.* **97**, 141–150.

Qiang, X. M., Cai, H. J. & Wang, J. 2009 Comparative study of crop evapotranspiration measured by Bowen ratio and lysimeter. *Trans. CSAE* **25** (2), 12–17 (in Chinese).

Qin, X. Y., Li, F., Chen, X. S. & Xie, Y. H. 2013 Growth responses and non-structural carbohydrates in three wetland macrophyte species following submergence and de-submergence. *Acta Physiol. Plant.* **35** (7), 2069–2074.

Refsgaard, J. C. & Storm, B. 1995 *MIKE SHE Computer Models in Watershed Hydrology.* Water Resources Publications, Littleton, CO, USA, pp. 809–846.

Ritchie, J. T. 1972 Model for predicting evaporation from a row crop with incomplete cover. *Water Resour. Res.* **8** (5), 1204–1213.

Sanderson, J. S. & Cooper, D. J. 2008 Ground water discharge by evapotranspiration in wetlands of an arid intermountain basin. *J. Hydrol.* **351** (3–4), 344–359.

Satchithanantham, S., Krahn, V., Ranjan, R. S. & Sager, S. 2014 Shallow groundwater uptake and irrigation water redistribution within the potato root zone. *Agric. Water Manage.* **132**, 101–110.

Schaap, M. G., Leij, F. J. & van Genuchten, M. T. H. 2001 ROSETTA: a computer program for estimating soil hydraulic parameters with hierarchical pedotransfer functions. *J. Hydrol.* **251** (3–4), 163–176.

Schlegel, P., Huwe, B. & Teixeira, W. G. 2004 Modelling species and spacing effects on root zone water dynamics using Hydrus-2D in an Amazonian agroforestry system. *Agroforest. Syst.* **60** (3), 277–289.

Sepaskhah, A. R. & Karimi-Goghari, S. 2005 Shallow groundwater contribution to pistachio water use. *Agric. Water Manage.* **72** (1), 69–80.

Sepaskhah, A. R., Kanooni, A. & Ghasemi, M. M. 2003 Estimating water table contributions to corn and sorghum water use. *Agric. Water Manage.* **58** (1), 67–79.

Shah, N., Nachabe, M. & Ross, M. 2007 Extinction depth and evapotranspiration from ground water under selected land covers. *Ground Water* **45** (3), 329–338.

Šimůnek, J., van Genuchten, M. T. H. & Šejna, M. 2008 *The HYDRUS-1D Software Package for Simulating the Movement of Water, Heat, and Multiple Solutes in Variably Saturated Media, Version 4.0.* Department of Environmental Sciences, University of California Riverside, Riverside, CA, USA.

Skaggs, T. H., Shouse, P. J. & Poss, J. A. 2006a Irrigating forage crops with saline waters: 2. Modeling root uptake and drainage. *Vadose. Zone. J.* **5** (3), 824–837.

Skaggs, T. H., van Genuchten, M. T., Shouse, P. J. & Poss, J. A. 2006b Macroscopic approaches to root water uptake as a function of water and salinity stress. *Agric. Water Manage.* **86** (1–2), 140–149.

Sommer, R., Folster, H., Vielhauer, K., Carvalho, E. J. M. & Vlek, P. L. G. 2003 Deep soil water dynamics and depletion by secondary vegetation in the eastern Amazon. *Soil. Sci. Soc. Am. J.* **67** (6), 1672–1686.

Sorrell, B. K., Tanner, C. C. & Brix, H. 2012 Regression analysis of growth responses to water depth in three wetland plant species. *AoB Plants* **2012**, pls043.

Soylu, M. E., Istanbulluoglu, E., Lenters, J. D. & Wang, T. 2011 Quantifying the impact of groundwater depth on evapotranspiration in a semi-arid grassland region. *Hydrol. Earth Syst. Sci.* **15** (3), 787–806.

Tan, Z. Q., Zhang, Q., Li, M. F., Li, Y. L., Xu, X. L. & Jiang, J. H. 2016 A study of the relationship between wetland vegetation communities and water regimes using a combined remote sensing and hydraulic modeling approach. *Hydrol. Res.* **47** (S1), 278–292.

van Genuchten, M. T. H. 1980 A closed-form equation for predicting the hydraulic conductivity of unsaturated soils. *Soil. Sci. Soc. Am. J.* **44** (5), 892–898.

van Genuchten, M. T. H. 1987 *A Numerical Model for Water and Solute Movement in and below the Root Zone.* Research Report No. 121. US Salinity Lab, Riverside, CA, USA.

Vretare, V., Weisner, S. E. B., Strand, J. A. & Graneli, W. 2001 Phenotypic plasticity in *Phragmites australis* as a functional response to water depth. *Aquat. Bot.* **69** (2–4), 127–146.

Wang, X. Y. 2003 Study of the estimating methods for evapotranspiration in farmland. *Syst. Sci. Compr. Stud. Agric.* **19** (2), 1–4 (in Chinese).

Wilcox, D. A., Meeker, J. E., Hudson, P. L., Armitage, B. J., Black, M. G. & Uzarski, D. G. 2002 Hydrologic variability and the application of index of biotic integrity metrics to wetlands: a Great Lakes evaluation. *Wetlands* **22** (3), 588–615.

Wu, G. P. & Liu, Y. B. 2015 Capturing variations in inundation with satellite remote sensing in a morphologically complex, large lake. *J. Hydrol.* **523**, 14–23.

Wu, Y. H. & Ji, W. T. 2002 *Study of Jiangxi Poyang Lake Nature Reserve.* China Forestry Press, Beijing, China (in Chinese).

Wu, J. D., Liu, G. H., Jin, J. F., You, X., Zhan, H. Y., Jia, W. M., Cao, R., Gao, Y. Y., Luo, H. & Gao, X. 2010 Structure analysis of beach vegetation in Poyang lake in autumn. *Jiangxi Sci.* **28** (4), 549–554 (in Chinese).

Xie, T., Liu, X. H. & Sun, T. 2011 The effects of groundwater table and flood irrigation strategies on soil water and salt dynamics and reed water use in the Yellow River Delta, China. *Ecol. Modell.* **222** (2), 241–252.

Xu, X. L., Zhang, Q., Li, Y. L., Li, X. H. & Wang, X. L. 2014 Annual variations of soil water content and groundwater level in a

typical islet wetland of Poyang Lake. *J. Lake. Sci.* **26** (2), 260–268 (in Chinese).

Xu, X. L., Zhang, Q., Tan, Z. Q., Li, Y. L. & Wang, X. L. 2015 Effects of water-table depth and soil moisture on plant biomass, diversity, and distribution at a seasonally flooded wetland of Poyang Lake, China. *Chin. Geog. Sci.* **25** (4), 739–756.

Yang, J. F., Wan, S. Q., Deng, W. & Zhang, G. X. 2007 Water fluxes at a fluctuating water table and groundwater contributions to wheat water use in the lower Yellow River floodplain, China. *Hydrol. Processes* **21** (6), 717–724.

Ye, X. C., Zhang, Q., Bai, L. & Hu, Q. 2011 A modeling study of catchment discharge to Poyang Lake under future climate in China. *Quat. Int.* **244** (2), 221–229.

Yu, L., He, L. H., Zhang, Q. & Wang, X. L. 2010 Landsat TM data based study on dynamic changes of the typical wetlands of Poyang Lake. *Remote Sens. Appl.* **6**, 48–54 (in Chinese).

Zhang, Y. K. & Schilling, K. E. 2006 Effects of land cover on water table, soil moisture, evapotranspiration, and groundwater recharge: a field observation and analysis. *J. Hydrol.* **319** (1–4), 328–338.

Zhang, G. X., Yin, X. R. & Feng, X. Q. 2008 Review of the issues related to wetland hydrology research. *Wetland Sci.* **6** (2), 105–115 (in Chinese).

Zhang, L. L., Yin, J. X., Jiang, Y. Z. & Wang, H. 2012a Relationship between the hydrological conditions and the distribution of vegetation communities within the Poyang Lake National Nature Reserve, China. *Ecol. Inf.* **11**, 65–75.

Zhang, Q., Li, L., Wang, Y. G., Werner, A. D., Xin, P., Jiang, T. & Barry, D. A. 2012b Has the Three-Gorges Dam made the Poyang Lake wetlands wetter and drier? *Geophys. Res. Lett.* **39** (20), L20402.

Zhang, Q., Ye, X. C., Werner, A. D., Li, Y. L., Yao, J., Li, X. H. & Xu, C. Y. 2014 An investigation of enhanced recessions in Poyang Lake: comparison of Yangtze River and local catchment impacts. *J. Hydrol.* **517**, 425–434.

Zhong, Z., Wu, Y. & Duan, M. 2014 Effects of low water level on Poyang Lake wetlands and migratory birds. *Jiangxi Hydraul. Sci. Technol.* **43** (3), 182–185 (in Chinese).

Zhou, W. B., Wan, J. B. & Jiang, J. H. 2011 *Impacts of Water Level Changes on Ecosystem in Poyang Lake.* Science Press, Beijing, China (in Chinese).

Zhu, Y. H., Ren, L. L., Skaggs, T. H., Lu, H. S., Yu, Z. B., Wu, Y. Q. & Fang, X. Q. 2009 Simulation of *populus euphratica* root uptake of groundwater in an arid woodland of the Ejina Basin, China. *Hydrol. Processes* **23** (17), 2460–2469.

First received 23 December 2015; accepted in revised form 14 July 2016. Available online 22 August 2016